

Mixed phase in a compact star with strong magnetic field

Ritam Mallick^a & P K Sahu^b

Institute of Physics, Sachivalaya Marg, Bhubaneswar 751005, INDIA

(Dated: October 13, 2018)

Abstract

Compact stars can have either hadronic matter or can have exotic states of matter like strange quark matter or color superconducting matter. Stars also can have a quark core surrounded by hadronic matter, known as hybrid stars (HS). The HS is likely to have a mixed phase in between the hadron and quark phase. Observational results suggest huge surface magnetic field in certain neutron stars (NS) called magnetars. Here we study the effect of strong magnetic field on the respective EOS of matter under extreme conditions. We further study the hadron-quark phase transition in the interiors of NS giving rise to hybrid stars (HS) in presence of strong magnetic field. The hadronic matter EOS is described based on relativistic mean field theory and we include the effect of strong magnetic fields leading to Landau quantization of the charged particles. For the quark phase we use the simple MIT bag model. We assume density dependent bag pressure and magnetic field. The magnetic field strength increases going from the surface to the center of the star. We construct the intermediate mixed phase using Glendenning conjecture. The magnetic field softens the EOS of both the matter phases. The effect of magnetic field is insignificant unless the field strength is above 10^{14} G. A varying magnetic field, with surface field strength of 10^{14} G and the central field strength of the order of 10^{17} G has significant effect on both the stiffness and the mixed phase regime of the EOS. We finally study the mass-radius relationship for such type of mixed HS, calculating their maximum mass, and compare them with the recent observation of pulsar PSR J1614-2230, which is about 2 solar mass. The observations puts a severe constraint on the EOS of matter at extreme conditions. The maximum mass with our EOS can reach the limit set by the observation.

PACS numbers: 26.60.Kp, 52.35.Tc, 97.10.Cv

^a Email:ritam.mallick5@gmail.com

^b Email:pradip@iopb.res.in

INTRODUCTION

The central density of neutron stars exceed the nuclear saturation density ($n_0 \sim 0.15\text{fm}^{-3}$), thereby raising the idea that compact stars might contain deconfined and chirally restored quark matter in them. Recently, [1] the mass measurement of millisecond pulsar PSR J1614-2230 has set a new robust mass limit for compact stars to be $M = 1.97 \pm 0.04 M_\odot$. This value, together with the mass of pulsar J1903+0327 of $M = 1.667 \pm 0.021 M_\odot$ [2] is much larger than any of the highest precisely measured pulsar mass. These measurement has set for the first time a very strong limit on parameters of the EOS, which describes matter under extreme conditions [3, 4].

After the discovery of pulsar [5] and connecting them with NS [6], various EOS for nuclear matter has been proposed and refined [7–10]. The quark sector is not much well understood as the nature of strong interaction at extreme condition still remains a challenge. The strange quark matter (SQM) conjecture by Itoh, Witten [11, 12] consisting of almost equal number of up (u), down (d) and strange (s) quarks was supported by model calculations [13]. The most simple and popular model which describes the properties of quark matter at such high densities is the MIT bag model [14]. New refined models based on results from recent experiments in laboratories has been proposed [15–17]. Thus normal nuclear matter at high density and/or temperature is likely to be unstable against stable SQM and would eventually decay.

Compact objects therefore can be made of either nuclear matter or quark matter. Stars which has only nuclear matter are called neutron stars (NS). Broadly there can be two classes of compact stars with quark matter. The first is the so-called (strange) quark stars (SS) of absolutely stable strange quark matter. The second are the so-called hybrid stars (HS), along with the hadronic matter they have quarks matter in their interior either in form of a pure strange quark matter core or color superconducting matter. In between the quark and the hadronic phase a quark-hadron mixed phase exists. The size of the core depends on the critical density for the quark-hadron phase transition and the EOS describing the matter phases.

Usually, the presence of strangeness in quark and hadronic matter provides an additional degree of freedom and softens the EOS and therefore quark and hybrid stars cannot reach high masses. Thus the mass measurement of pulsar PSR J1614-2230 puts forward a strong

constraint on such EOS. However, studies found that effects from the strong interaction, such as one-gluon exchange or color-superconductivity can stiffen the quark matter EOS and increase their maximum mass [18–23]. The first studies on the implications of the new mass limits from PSR J1614-2230 for quark matter was done by [24] and [25]. They, however did not include the effects from color-superconductivity.

The presence of magnetic field in compact stars has an important role in astrophysics. New observations suggests that in some pulsars the surface magnetic field can be as high as $10^{14} - 10^{15}$ G. It has also been attributed that the observed giant flares, SGR 0526-66, SGR 1900+14 and SGR 1806-20 [26], are the manifestation of such strong surface magnetic in those stars. Such stars are separately assigned as magnetars. If we assume flux conservation from a progenitor star, we can expect the central magnetic field of such stars as high as $10^{17} - 10^{18}$ G. Such strong fields are bound to effect the NS properties. It can modify the metric describing the star [27, 28] or it can modify the EOS of matter of the star. The effect of strong magnetic field, both for nuclear matter [29, 30, 32–34] and quark matter [35–37] has been studied earlier in detail.

Motivated by recent observations of maximum mass limits of compact stars and strong magnetic field in magnetars, in this work we want to explore their implications on the EOS of both phases of matter that may be present inside a neutron star. We study the hadron-quark phase transition inside a compact star with a mixed phase region in between the quark core and nuclear outer region. The paper is organized as follows. In Sec. II we discuss the nuclear EOS and the effect of Landau quantization due to magnetic field on the charged particles. In Sec. III we employ the simple MIT bag model for the quark matter EOS and the effect of magnetic field on the quarks (also due to Landau quantization). In Section IV we develop the mixed phase region by Glendenning construction. We show our results in section V for the density dependent bag constant and varying magnetic field for the mixed HS. Finally we summarize our results and draw some conclusion in section VI.

MAGNETIC FIELD IN HADRONIC PHASE

At normal nuclear density the degrees of freedom for the EOS are hadrons. To describe the hadronic phase, we use a non-linear version of the relativistic mean field (RMF) model with hyperons (TM1 parametrization) which is widely used to construct EOS for NS. In this

model the baryons interact with mean meson fields [38–43].

The Lagrangian density including nucleons, baryon octet ($\Lambda, \Sigma^{0,\pm}, \Xi^{0,-}$) and leptons is given by

$$\begin{aligned}
\mathcal{L}_H = & \sum_b \bar{\psi}_b [\gamma_\mu (i\partial^\mu - g_{\omega b}\omega^\mu - \frac{1}{2}g_{\rho b}\vec{\tau}\cdot\vec{\rho}^\mu) \\
& - (m_b - g_{\sigma b}\sigma)] \psi_b + \frac{1}{2}(\partial_\mu\sigma\partial^\mu\sigma - m_\sigma^2\sigma^2) \\
& - \frac{1}{4}\omega_{\mu\nu}\omega^{\mu\nu} + \frac{1}{2}m_\omega^2\omega_\mu\omega^\mu - \frac{1}{4}\vec{\rho}_{\mu\nu}\cdot\vec{\rho}^{\mu\nu} \\
& + \frac{1}{2}m_\rho^2\vec{\rho}_\mu\cdot\vec{\rho}^\mu - \frac{1}{3}bm_n(g_\sigma\sigma)^3 - \frac{1}{4}c(g_\sigma\sigma)^4 + \frac{1}{4}d(\omega_\mu\omega^\mu)^2 \\
& + \sum_L \bar{\psi}_L [i\gamma_\mu\partial^\mu - m_L]\psi_L.
\end{aligned} \tag{1}$$

Leptons \mathcal{L} are treated as non-interacting and baryons b are coupled to the scalar meson σ , the isoscalar-vector meson ω_μ and the isovector-vector meson ρ_μ . There are five constants in the model that are fitted to the bulk properties of nuclear matter. This model is good enough to describe nuclear matter and the nuclear saturation point. But it is insufficient for the hyperonic matter, because the model does not reproduce the observed strong $\Lambda\Lambda$ attraction. This defect can be remedied by adding two new meson fields with hidden strangeness, namely, the iso-scalar scalar σ^* and the iso-vector vector ϕ , which couple to hyperons only [42].

The effective baryon mass is given by

$$m_b^* = m_b - g_\sigma\sigma - g_{\sigma^*}\sigma^*. \tag{2}$$

For the beta equilibrated matter the conditions is

$$\mu_i = b_i\mu_B + q_i\mu_e, \tag{3}$$

where b_i and q_i are the baryon number and charge (in terms of electron charge) of species i , respectively. μ_B is the baryon chemical potential and μ_e is the electron chemical potential.

For charge neutrality, the condition is

$$\rho_c = \sum_i q_i n_i, \tag{4}$$

n_i is the baryon number density of particle i .

The magnetic field is assumed to be in the z direction, $\vec{B} = B\hat{k}$. Now the motion of the charged particles are quantized in the perpendicular direction of the magnetic field. The

landau quantized energy is given by [44]

$$E_i = \sqrt{p_i^2 + m_i^2 + |q_i|B(2n + s + 1)}. \quad (5)$$

In the above equation n is the principle quantum number, s is the spin of the particle (either (+) or (-)) and p_i is the momentum component along the field direction of particle i . We can write $2n + s + 1 = 2\nu$, where $\nu = 0, 1, 2, \dots$, so that now the energy can be written as

$$E_i = \sqrt{p_i^2 + m_i^2 + 2\nu|q_i|B} = \sqrt{p_i^2 + \widetilde{m}_{i,\nu}^2} \quad (6)$$

where the $\nu = 0$ state is singly degenerate. It should be remembered that for baryons the mass is m_b^* .

At zero temperature and in the presence of a constant magnetic field B , the number and energy densities of charged particles are given by [29, 35]

$$n_i = \frac{|q_i|B}{2\pi^2} \sum_{\nu} p_{f,\nu}^i, \quad (7)$$

and

$$\varepsilon_i = \frac{|q_i|B}{4\pi^2} \sum_{\nu} \left[E_f^i p_{f,\nu}^i + \widetilde{m}_{\nu}^i{}^2 \ln \left(\left| \frac{E_f^i + p_{f,\nu}^i}{\widetilde{m}_{\nu}^i} \right| \right) \right]. \quad (8)$$

$p_{f,\nu}^i$ is the Fermi momentum for the level with the principal quantum number n and spin s and is given by

$$p_{f,\nu}^i{}^2 = E_f^i{}^2 - \widetilde{m}_{\nu}^i{}^2. \quad (9)$$

The Fermi energies are fixed by their respective chemical potentials.

The number, energy, and scalar number densities of the neutral particles are given by

$$n_N = \frac{p_f^N{}^3}{3\pi^2}, \quad (10)$$

$$n_N^s = \frac{m_N^*}{2\pi^2} \left[E_f^N p_f^N - m_N^*{}^2 \ln \left(\left| \frac{E_f^N + p_f^N}{m_N^*} \right| \right) \right], \quad (11)$$

$$\varepsilon_N = \frac{1}{8\pi^2} \left[2E_f^N{}^3 p_f^N - m_N^*{}^2 E_f^N p_f^N - m_N^*{}^4 \ln \left(\left| \frac{E_f^N + p_f^N}{m_N^*} \right| \right) \right]. \quad (12)$$

The total energy density of the system can be written as

$$\begin{aligned} \varepsilon = & \frac{1}{2}m_{\omega}^2\omega_0^2 + \frac{1}{2}m_{\rho}^2\rho_0^2 + \frac{1}{2}m_{\sigma}^2\sigma^2 + \frac{1}{2}m_{\sigma^*}^2\sigma^{*2} + \frac{1}{2}m_{\phi}^2\phi_0^2 + \frac{3}{4}d\omega_0^4 + U(\sigma) \\ & + \sum_b \varepsilon_b + \sum_l \varepsilon_l + \frac{B^2}{8\pi^2}, \end{aligned} \quad (13)$$

where the last term is the contribution from the magnetic field. The general expression for the pressure is given by

$$P = \sum_i \mu_i n_i - \varepsilon. \quad (14)$$

At the outermost surface of the star, that is at lower densities, the matter is composed of only neutrons, protons and electrons. Hence, at the low density regime, only the electrons and protons are affected by the magnetic field. Electron being highly relativistic, the number of occupied Landau levels by electrons is very large. The field strength under consideration is larger than the critical field strength of electron by several orders but very less than the critical field strength of protons. Therefore, the number of occupied Landau levels by protons is large. As the magnetic field increases with the increase of density, the number of occupied Landau levels gradually decreases for every species.

MAGNETIC FIELD IN QUARK PHASE

Considering the simple MIT bag model for the quark matter in presence of magnetic field we assume that the quarks are non-interacting. The current masses of u and d quarks are extremely small, e.g., 5 and 10 MeV respectively, whereas, for s-quark the current quark mass is taken to be 150 MeV, unless otherwise stated.

For the same constant magnetic field configuration along the z-axis, the single energy eigenvalue is given by[44]

$$E_i = \sqrt{p_i^2 + m_i^2 + 2\nu|q_i|B} \quad (15)$$

Then the thermodynamic potential in presence of strong magnetic field $B(> B^{(c)}$, critical value discussed later) is given by [45]

$$\Omega_i = -\frac{g_i|q_i|BT}{4\pi^2} \int dE_i \sum_{\nu} \frac{dp_i}{dE_i} \ln[1 + \exp(\mu_i - E_i)/T]. \quad (16)$$

For the zero temperature, the Fermi distribution is approximated by a step function and by interchanging the order of the summation over ν and integration over E ,

$$\Omega_i = -\frac{2g_i|q_i|B}{4\pi^2} \sum_{\nu} \int_{\sqrt{m_i^2+2\nu|q_i|B}}^{\mu} dE_i \sqrt{E_i^2 - m_i^2 - 2\nu|q_i|B}. \quad (17)$$

The upper limit of ν sum can be obtained from the following relation

$$p_{f,i}^2 = \mu_i^2 - m_i^2 - 2\nu|q_i|B \geq 0, \quad (18)$$

where $p_{f,i}$ is the Fermi momentum of the particle i .

The upper limit is not necessarily same for all the components. For a certain critical magnetic field strength the energy of a charged particle changes significantly in the quantum limit. For an electron with mass 0.5 MeV, the critical field strength is $\sim 4.4 \times 10^{13}\text{G}$, whereas for a light quark (u or d), this value becomes $\sim 4.4 \times 10^{15}\text{G}$, and for s-quark of current mass 150 MeV, it is $\sim 10^{19}\text{G}$. A compact star becomes unstable if the magnetic field strength becomes much greater than $\sim 10^{18}\text{G}$, and so many authors have neglected quantum mechanical effect of magnetic field on s-quarks [46] but in our calculation we include the quantum mechanical effect for all particles.

Assuming the strange quark matter also to be charge neutral and in chemical equilibrium, we may write as

$$\mu_d = \mu_s = \mu = \mu_u + \mu_e, \quad (19)$$

$$2n_u - n_d - n_s - 3n_e = 0. \quad (20)$$

The baryon number density is given by

$$n_b = \frac{1}{3}(n_u + n_d + n_s). \quad (21)$$

Solving the above eqs(19, 20, 21) numerically, we obtain the chemical potentials of all the flavors and electron. Zero temperature approximation gives the number density of the species i (u, d, s, e)

$$n_i = \frac{g_i |q_i| B}{4\pi^2} \sum_{\nu} \sqrt{\mu_i^2 - m_i^2 - 2\nu |q_i| B}. \quad (22)$$

The total energy density and pressure of the strange quark matter is given by

$$\begin{aligned} \varepsilon &= \sum_i \Omega_i + B_G + \sum_i n_i \mu_i \\ p &= - \sum_i \Omega_i - B_G, \end{aligned} \quad (23)$$

where B_G is the bag constant.

PHASE TRANSITION AND MIXED PHASE

With the above given hadronic and quark EOS, we now perform the Glendenning construction [47] for the mixed phase, which determines the range of baryon density where both phases coexist. Allowing both the hadron and quark phases to be separately charged, and

still preserving the total charge neutrality as a whole in the mixed phase. Thus the matter can be treated as a two-component system, and can be parametrized by two chemical potentials, usually the pair (μ_e, μ_n) , i.e., electron and baryon chemical potential. To maintain mechanical equilibrium, the pressure of the two phases are equal. Satisfying the chemical and beta equilibrium the chemical potential of different species are connected to each other. The Gibbs condition for mechanical and chemical equilibrium at zero temperature between both phases is given by

$$P_{\text{HP}}(\mu_e, \mu_n) = P_{\text{QP}}(\mu_e, \mu_n) = P_{\text{MP}}. \quad (24)$$

This equation gives the equilibrium chemical potentials of the mixed phase corresponding to the intersection of the two phases. At lower densities below the mixed phase, the system is in the charge neutral hadronic phase, and for higher densities above the mixed phase the system is in the charge neutral quark phase. As the two surfaces intersect, one can calculate the charge densities ρ_e^{HP} and ρ_e^{QP} separately in the mixed phase. If χ is the volume fraction occupied by quark matter in the mixed phase, we have

$$\chi\rho_e^{\text{QP}} + (1 - \chi)\rho_e^{\text{HP}} = 0. \quad (25)$$

Therefore the energy density ϵ_{MP} and the baryon density n_{MP} of the mixed phase can be obtained as

$$\epsilon_{\text{MP}} = \chi\epsilon_{\text{QP}} + (1 - \chi)\epsilon_{\text{HP}}, \quad (26)$$

$$n_{\text{MP}} = \chi n_{\text{QP}} + (1 - \chi)n_{\text{HP}}. \quad (27)$$

RESULTS

In neutron stars, the central part of the star has maximum density, therefore, it is much likely that the matter there undergoes a phase transition. As the density decreases towards the surface there is a probability of having nuclear matter and so in the intermediate stage there is a mixed phase, and as we go outwards we only have nuclear matter. The crust consisting mainly free electrons and nuclei which completes the star structure.

The parametrization of the EOS of the hadron and quark phase is responsible for characterization of the mixed phase region. For the hadronic EOS we assume a fixed parameter set TM1, which reproduces the nuclear matter properties at high density quite well. However

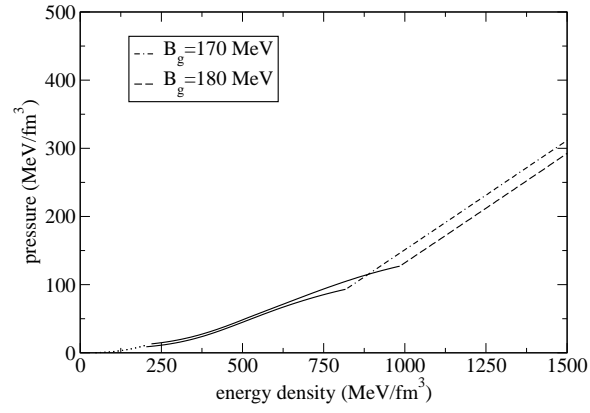


FIG. 1. Pressure vs energy density plot with bag pressure of 170 and 180MeV.

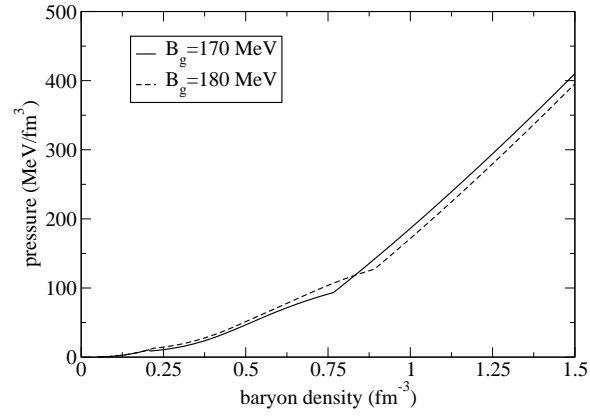


FIG. 2. Pressure vs number density plot with bag pressure of 170 and 180MeV.

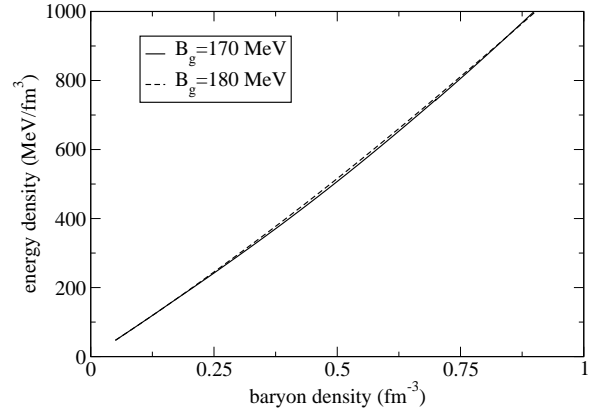


FIG. 3. Energy density vs number density plot with bag pressure of 170 and 180MeV.

the quark EOS can be controlled by changing the quark masses and the bag constant. The masses of the light quarks (u and d) are bounded and we take them to be 5 and 10MeV, respectively. The mass of s-quark is still not established, and can vary between 100 – 300MeV, and we take them to be 150MeV, unless otherwise stated. We regulate the bag constant (B_G) to characterize the mixed phase region. Now we use the Glendenning approach to construct the mixed phase, and obtain pressure vs energy density relation as given in fig 1. In fig 1, we have plotted the mixed phase EOS (pressure vs energy) with bag pressure 170 and 180MeV. For simplicity, we will denote $B_G^{1/4} = 170MeV = B_g$. The lower portion of the curve is nuclear phase (dotted line), the intermediate portion is the mixed phase (bold line) and the upper region is the quark phase (broken line). The curve with bag constant 170MeV is much stiffer than the curve with bag pressure 180MeV, because the bag pressure is negative to the matter pressure, making the effective pressure less. In fig 2 we have plotted pressure vs number density, and we find that the qualitative variation in the curves is same as that of fig 1. For bag constant 170MeV the mixed phase region starts at density $0.2fm^{-3}$ and ends at $0.76fm^{-3}$. With bag constant 180MeV the mixed phase region starts at density $0.22fm^{-3}$ and ends at $0.89fm^{-3}$. In fig 3 we have plotted for the energy density vs number density, and we find a smooth curve, which does not differ from each other much. It is clear from the above figures that the main variation is due to the pressure, therefore, we only plot the pressure vs energy density curve. The above curves shows that as the bag pressure increases the range of mixed phase region increases, and there is a slight kink in the curve from going to the quark phase from the mixed phase. The EOS (or the pressure) for the nuclear matter is usually much stiffer than quark matter. As the bag constant with 170 MeV is more stiffer than 180MeV the kink in the former is much sharper than the latter one. Also as the latter curve is much flatter and so the mixed phase region is much extended there. By the Glendenning construction, we find that for a given mixed phase to exist the bag constant must be in between 170MeV and 180 MeV.

The introduction of the magnetic field changes the EOS of the matter. The single particle energy is now Landau quantized, and thereby it changes all the other thermodynamic variable of the EOS, namely the number density, pressure and the energy density. In fig 4, we have plotted EOS for bag constant 170MeV with and without the magnetic field. The effect of magnetic field is insignificant when the field strength is less than $10^{14}G$, and also for this case the effect in the nuclear phase is very small. The magnetic field effect is less for the

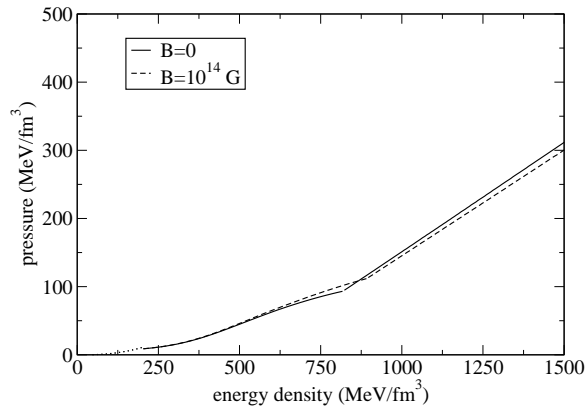


FIG. 4. Pressure against energy density plot with bag pressure of 170MeV with and without magnetic field. The magnetic field is $B = 10^{14}$ G.

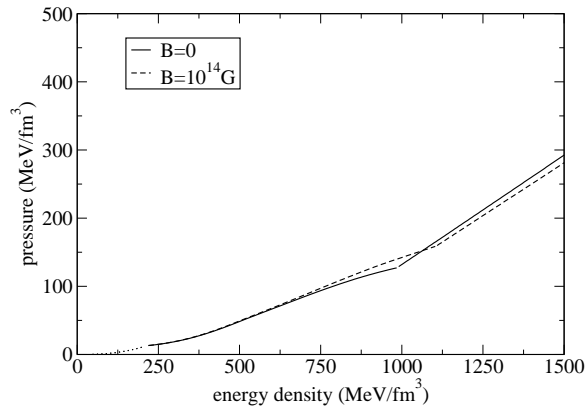


FIG. 5. Pressure against energy density plot with bag pressure of 180MeV with and without magnetic field. The magnetic field is $B = 10^{14}$ G.

nuclear matter than quark matter because, the nuclear EOS is much steeper than the quark EOS, thereby requiring much greater field to have any sound effect. We have plotted the same for bag constant 180MeV (fig 5), and for comparing the two bag constants, we have plotted fig 6. For the bag constant 170 MeV, the EOS curve with magnetic field extends up to density $0.8fm^{-3}$, and for 180 MeV it extends upto density $0.92fm^{-3}$. The change in the mixed phase region is about 5 – 7%. Magnetic field makes the curve softer due to the negative effect of landau quantization on the matter pressure and the positive effect on the matter energy density. As shown in the figures, the effect of magnetic field begins to appear on the EOS of the matter when the field strength is above 10^{14} G. Such field has very

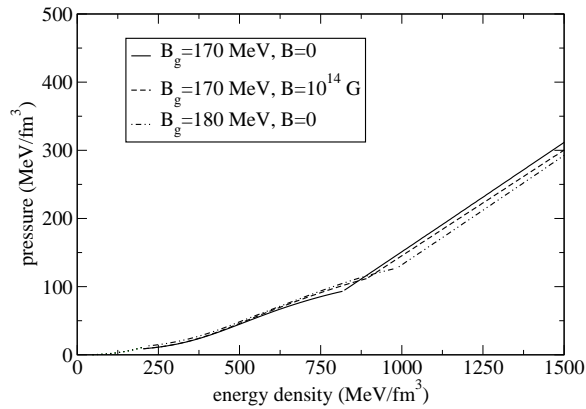


FIG. 6. Pressure against energy density plot with bag pressure of 170 and 180MeV. For the bag pressure 170MeV we have also plotted curve with magnetic field of strength 10^{14} G.

less effect on the nuclear matter but has considerable effect on the mixed and quark matter. With the onset of the magnetic field the mixed phase region gets extended. The magnetic field makes the quark matter EOS more flatter and therefore the mixed phase region is much extended. For fixed bag constant and fixed magnetic field value throughout, we cannot go to field strength above 10^{15} G, as it is bounded by observation of surface magnetic fields in magnetars.

Next we assume a density dependent bag constant. In the literature there are several attempts to understand the density dependence of bag constant [48, 49]; but still there is no definite picture, and most of them are model dependent. We parametrized the bag constant in such a way that it attains a value B_∞ , asymptotically at very high densities. The experimental range of B_∞ is given in Burgio et al. [50, 51], and from there we choose the value $B_\infty = 130$ MeV. With such assumptions we then construct a Gaussian parametrization given as [50, 51]

$$B_{gn}(n_b) = B_\infty + (B_g - B_\infty) \exp \left[-\beta \left(\frac{n_b}{n_0} \right)^2 \right]. \quad (28)$$

The lowest value B_∞ , is the lowest value of bag pressure which it attains at asymptotic high density in quark matter, and is fixed at 130MeV. The quoted value of bag pressure, is the value of the bag constant at the nuclear and mixed phase intersection point denoted by B_g in the equation. The value of B_{gn} decrease with increase in density and attain $B_\infty = 130$ MeV asymptotically, the rate of decrease of the bag pressure is governed by parameter β .

The observed magnetic field of the magnetars is of the order of $\sim 10^{14} - 10^{15}$ G. The flux

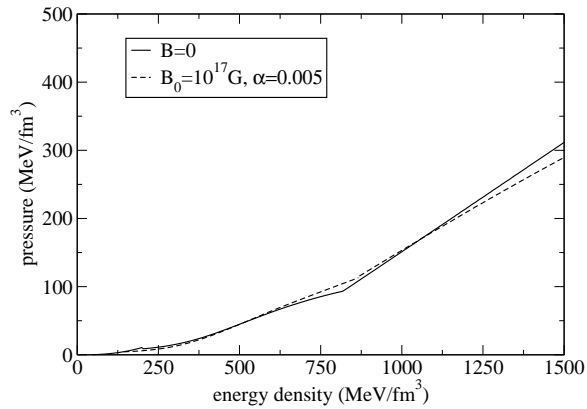


FIG. 7. Pressure as energy density plot with bag pressure of 170MeV, with and without varying magnetic field. The varying magnetic field has $B_0 = 10^{17}$ G and $\alpha = 0.005$.

conservation of the progenitor star may give the central field as high as $\sim 10^{17} - 10^{18}$ G. We assume that the parametrization of the magnetic field depends on the baryon number density. Therefore we assume a simple density dependence, given by [30, 31]

$$B(n_b) = B_s + B_0 \left\{ 1 - e^{-\alpha \left(\frac{n_b}{n_0} \right)^\gamma} \right\}, \quad (29)$$

where α and γ determines the magnetic field variation for fixed surface field B_s and asymptotic central field B_0 . The value of B depends mainly on B_0 , and is quite independent of B_s . Therefore we vary B_0 , whereas surface field strength is taken to be fixed at $B_s = 10^{14}$ G. We keep γ fixed at 2, and vary α for to have the field variation. Previous authors considered very high magnetic field value at the center, few times 10^{18} G, but we would assume the maximum field to be of the order of few 10^{17} G. As this is somewhat low value from other previous assumptions, but it is more likely to be present in most magnetars.

Next, we vary the magnetic field, and the bag constant is kept constant. First we consider the bag constant to be $B_g = 170$ MeV. In fig 7 we have plotted curves for zero magnetic field and with $B_0 = 10^{17}$ G with $\alpha = 0.005$. As we vary the magnetic field, the magnetic field increases as we go towards to the center of the star. The field quoted in the figure is asymptotic field value. With $B_0 = 10^{17}$ G and $\alpha = 0.005$, the field strength is 4×10^{16} G at $10n_0$. It is clear from the figure as the field strength increases, the curve becomes less stiffer. The change in the curve stiffness is due to the fact that the magnetic pressure due to landau quantization act in the opposite direction of the matter pressure, whereas, for the magnetic stress it acts towards the matter energy density. The two effect reduces the stiffness of

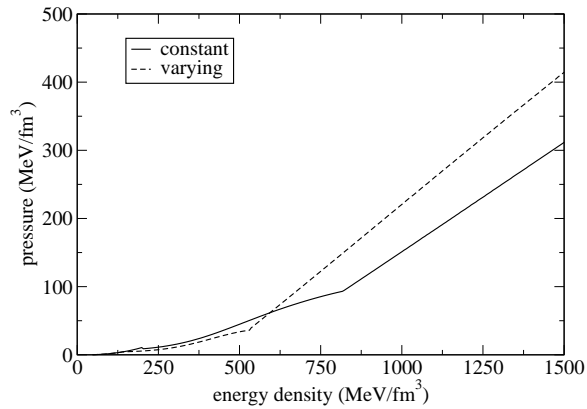


FIG. 8. Pressure against energy density plot with constant and varying bag pressure, $B_g = 170\text{MeV}$.

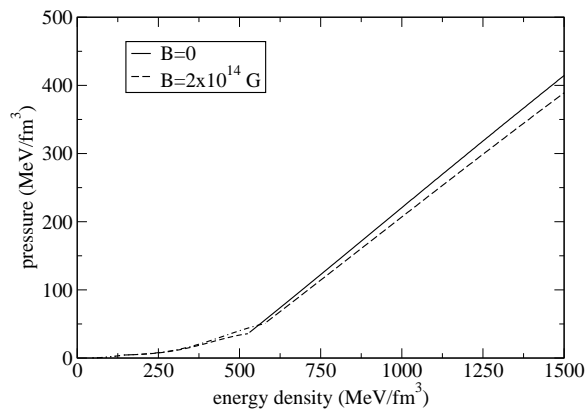


FIG. 9. Pressure against energy density plot having density dependent bag pressure $B_g = 170\text{MeV}$, with and without magnetic field. The magnetic field strength is $B = 2 \times 10^{14}\text{G}$.

the EOS (pressure vs energy density curve). It is also clear that the nuclear region (the low density regime) is not much affected by the magnetic field as there the magnetic field strength is low, whereas the quark sector (higher density regime) is the most effected region as the field strength is maximum there. However, the mixed phase region is moderately affected (the intermediate region).

In fig 8 we plot curves with and without varying bag pressure, $B_g = 170\text{MeV}$. For the curve with variation, at higher densities the bag pressure decreases, making the effective matter pressure higher. Therefore the pressure against energy density plot for this case is much stiffer. Also the mixed phase region gets shrunken due to the varying bag pressure.

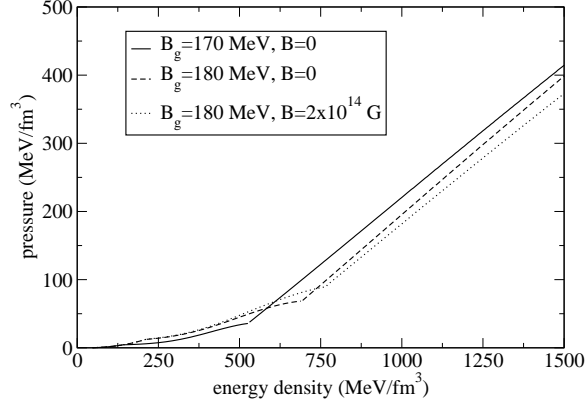


FIG. 10. Pressure against energy density plot having density dependent bag pressure $B_g = 170\text{MeV}$ and 180MeV . Also shown in the figure the magnetic field ($B = 2 \times 10^{14}\text{G}$) induced EOS curve for $B_g = 170\text{MeV}$.

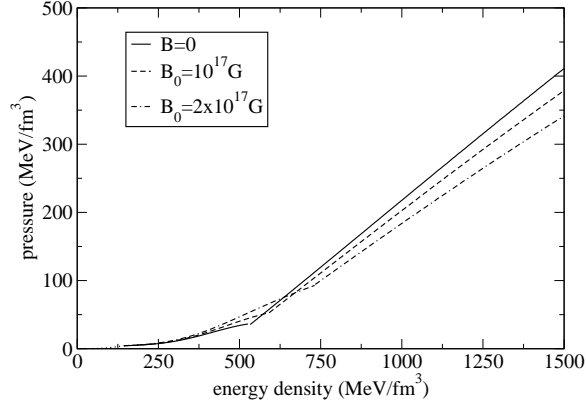


FIG. 11. Pressure with energy density plot having density dependent bag pressure 170MeV , without magnetic field and with two different magnetic fields, having $\alpha = 0.005$.

The mixed phase region now only extends up to density 0.53fm^{-3} . The change in the mixed phase region is about 40%. Therefore the change in the mixed phase region is much more influenced by varying bag pressure than due to magnetic field. We have plotted fig 9 with varying bag pressure $B_g = 170\text{MeV}$, with and without constant magnetic field. The magnetic field employed for this plot is $2 \times 10^{14}\text{G}$. The change in the slope of the curves is due to the Landau quantization effect. The magnetic pressure acts opposite to the matter pressure, making the curve flat. For comparison, we have plotted fig 10 with density dependent bag pressure, $B_g = 170$ and $B_g = 180\text{MeV}$, and obtain quantitative same result.

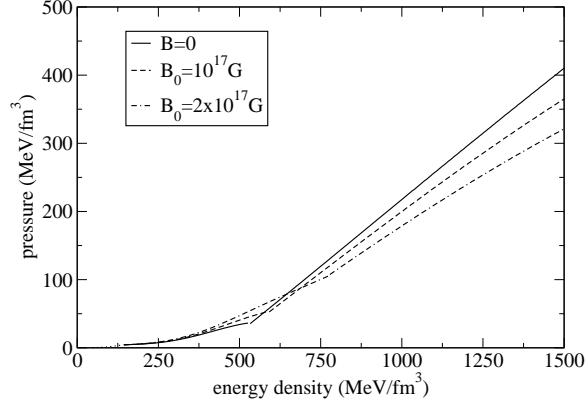


FIG. 12. Pressure with energy density plot having density dependent bag pressure 170MeV, without magnetic field and with two different magnetic fields, having $\alpha = 0.01$.

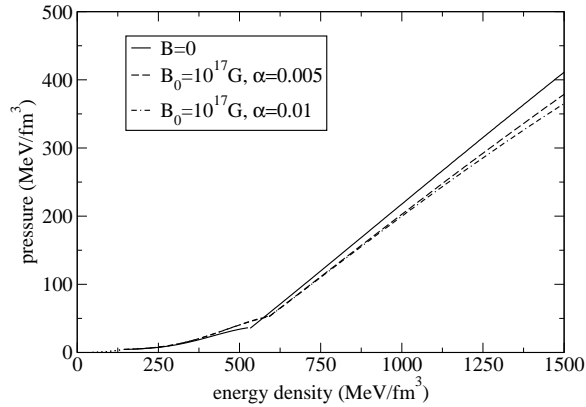


FIG. 13. Pressure with energy density plot having density dependent bag pressure 170MeV, without magnetic field and with same magnetic field but different α values.

The curves for which both the bag constant and the magnetic field varies are of utmost importance. Fig 11 shows curves for varying bag pressure 170MeV, without magnetic field and with varying magnetic field, $B_0 = 10^{17}\text{G}$ and $2 \times 10^{17}\text{G}$ having $\alpha = 0.005$. For the above values the field strength is $4 \times 10^{16}\text{G}$ and $7.8 \times 10^{16}\text{G}$, at density $10n_0$. As the value of B_0 increases the slope of the EOS curves becomes more and more soft, because the value of magnetic pressure increases with increase in field strength. As the magnetic pressure increases the effective pressure decreases making the curves flatter. In fig 12 we plot the same set of curve only for $\alpha = 0.01$. With such α value, the asymptotic $B_0 = 10^{17}\text{G}$ gives field strength of $6 \times 10^{16}\text{G}$ at $10n_0$ baryon density. For $B_0 = 2 \times 10^{17}\text{G}$ the field strength

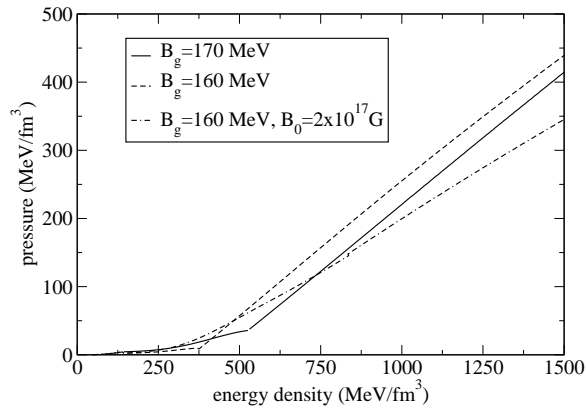


FIG. 14. Pressure vs energy density plot with two different density dependent bag pressure 160MeV, 170MeV. We have also plotted the magnetic field induced (field strength $B_0 = 2 \times 10^{17}$ G) EOS curve for bag pressure 160MeV having $\alpha = 0.01$.

is 1.21×10^{17} G at the same $10n_0$ baryon density. As the variation (α) becomes stiffer, the EOS curve becomes softer. This is seen clearly in fig 13.

We find for such varying bag constant and varying magnetic field, the change in the curves from the non varying non magnetic case is maximum. There is considerable change in the stiffness of the curves and also change in the mixed phase region. Towards the center, the magnetic field increases whereas the bag pressure decreases. On one hand the low bag pressure makes the curve stiffer whereas on the other hand large magnetic field strength makes the curve flatter. The low bag constant makes the mixed phase region to shrink, and the larger magnetic field tries to expand the mixed phase region. The effect of bag pressure is greater than the magnetic field and therefore the mixed phase is smaller than the constant bag pressure case. On the low density side, the effect of magnetic field is insignificant. Therefore the phase boundary between the nuclear and mixed phase is not much affected.

For a varying bag constant we can have a significant mixed phase region with $B_g = 160$ MeV (fig 14). The curve with bag pressure 160MeV is stiffer than other curves. This is because the bag pressure of $B_g = 160$ MeV is lower than other higher bag pressure. Therefore, the effective matter pressure for this curve is higher than any other curve, which is reflected in the stiffness of the curve. For bag constant 160MeV the mixed phase region starts at density $0.15 fm^{-3}$ and ends at $0.38 fm^{-3}$.

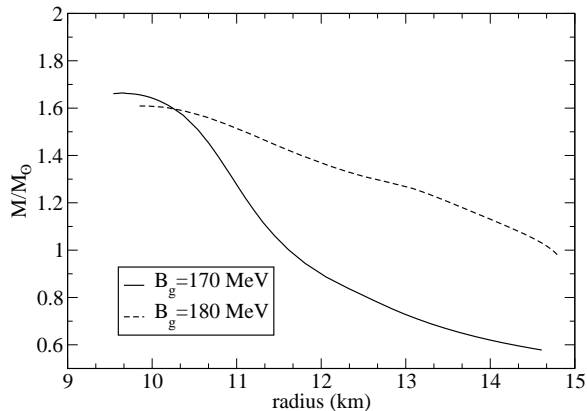


FIG. 15. Gravitational mass (in solar mass) against radius plot of a star sequence with two different density dependent bag pressure, 170 and 180MeV.

Assuming the star is non rotating and has spherically symmetric, the distribution of mass is in hydrostatic equilibrium. The equilibrium configurations solution are obtained by solving the Tolman-Oppenheimer-Volkoff (TOV) equations [52] for the pressure $P(\epsilon)$ and the enclosed mass m ,

$$\frac{dP(r)}{dr} = -\frac{Gm(r)\epsilon(r)}{r^2} \frac{[1 + P(r)/\epsilon(r)] [1 + 4\pi r^3 P(r)/m(r)]}{1 - 2Gm(r)/r}, \quad (30)$$

$$\frac{dm(r)}{dr} = 4\pi r^2 \epsilon(r), \quad (31)$$

G is the gravitational constant. Starting with a central energy density $\epsilon(r = 0) \equiv \epsilon_c$, we integrate out until the pressure on the surface equals the one corresponding to the density of iron. This gives the stellar radius R and the total gravitational mass is then

$$M_G \equiv m(R) = 4\pi \int_0^R dr r^2 \epsilon(r). \quad (32)$$

For the description of the NS crust, we have added the hadronic equations of state with the ones by Negele and Vautherin [53] in the medium-density regime, and the ones by Feynman-Metropolis-Teller [54] and Baym-Pethick-Sutherland [55] for the outer crust.

Fig 15 shows the gravitational mass M (in units of solar mass M_\odot) as a function of radius R , for varying bag pressure $B_g = 170$ and 180 MeV. As the bag pressure increases the curve becomes flatter as the effective matter pressure decreases (bag pressure being negative) thereby decreasing the maximum mass of the star. We notice that a flatter EOS corresponds to a flatter mass-radius curve. Next we plot fig 16, with constant bag pressure of 170MeV,

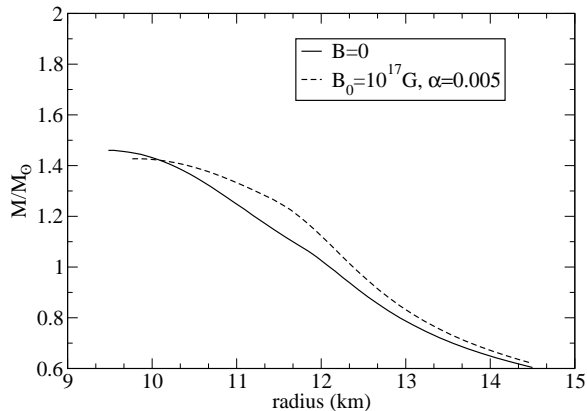


FIG. 16. Gravitational mass (in solar mass) with radius plot of a star sequence with constant bag pressure of 170MeV, without magnetic field and with varying magnetic field of field strength $B_0 = 10^{17}\text{G}$ and $\alpha = 0.005$.

with and without magnetic field. The mass vs radius curve in fig 16 is flatter than fig 15 because this corresponds to the EOS for constant bag pressure, which is much flatter than the EOS with varying bag pressure. The varying magnetic field has $B_0 = 10^{17}\text{G}$ and $\alpha = 0.005$. Initially, the mass for the star with magnetic field is higher, but the maximum mass is lower than the non magnetic case, because the non magnetic EOS is steeper than the magnetic counterpart. The stiffness (or flatness) of the pressure vs energy density curve for a particular EOS is reflected in the stiffness (or flatness) of the corresponding mass-radius curve.

Next in fig 17, we plot curves with varying bag constant (170MeV) for two different value of alpha (0.005 and 0.01), with field strength of $B_0 = 2 \times 10^{17}\text{G}$. Both the magnetic field and bag pressure are density dependent. The magnetic field makes the mass-radius curve flatter. As the magnetic field variation becomes higher, increasing the magnetic field strength as we go inwards, and thereby making the EOS flat. As the EOS becomes flat the mass-radius curve also becomes flat, and the maximum mass decreases. To compare the mass dependence on varying magnetic field and varying bag pressure we have plotted curves for two different set of curves with varying bag pressure 170 and 180MeV (fig 18). Each set comprising of two curves one without magnetic field and one with magnetic field, of strength $B_0 = 2 \times 10^{17}\text{G}$. The qualitative nature of the curves remains same due the reasons discussed earlier. As it has been pointed out, with varying bag constant and varying magnetic field we can have

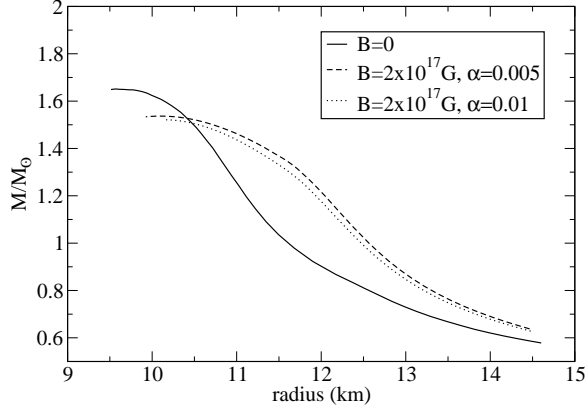


FIG. 17. Gravitational mass (in solar mass) with radius plot of a star sequence having density dependent bag pressure 170MeV. Curves are plotted without magnetic field and with same magnetic field, of field strength $B_0 = 2 \times 10^{17} \text{G}$ but different α .

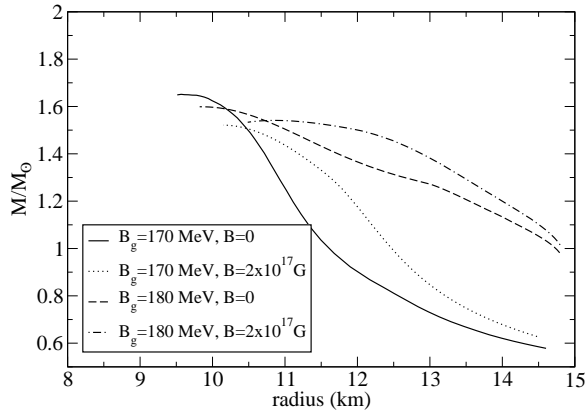


FIG. 18. Gravitational mass (in solar mass) against radius plot of a star sequence with two different varying bag pressure of 170MeV and 180MeV. The curves are plotted without magnetic field and with magnetic field, of strength $B_0 = 2 \times 10^{17} \text{G}$ having same $\alpha = 0.01$.

mixed phase EOS with bag pressure of 160MeV. In fig 19, we have plotted the mass-radius curve for $B_g = 160 \text{MeV}$, with ($B_0 = 2 \times 10^{17} \text{G}$) and without magnetic field. The magnetic field is varying having α of 0.01. The maximum mass for this case is obtained without the magnetic field effect and the introduction of the magnetic field makes the curve flatter and also reduces the maximum mass. The maximum mass of a mixed hybrid star obtained with such mixed phase region is $1.84M_\odot$.

Recently, after the discovery of high-mass pulsar PSR J1614-2230 [1] with mass of about

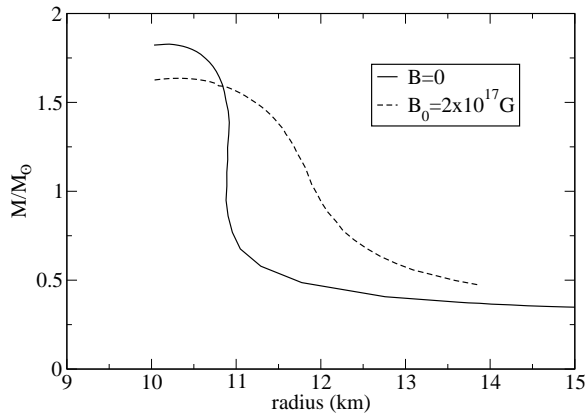


FIG. 19. Gravitational mass (in solar mass) against radius plot of a star sequence with density dependent bag pressure of 160MeV. Two curves are plotted, one without magnetic field and one with magnetic field, having strength $B_0 = 2 \times 10^{17}$ G and $\alpha = 0.01$.

$1.97M_\odot$, the EOSs describing the interior of a compact star have been put to severe constraint. The [1] typical values of the central density of J1614-2230, for the allowed EOSs is in the range $2n_0 - 5n_0$. On the other hand, consideration of the EOS independent analysis of [56] sets the upper limit of central density at $10n_0$. For a constant bag pressure, the mass of the HS is about 1.5 solar mass (fig 16). With a varying bag pressure, the maximum mass limit can be increased. The maximum mass limit of mixed phase EOS star with the above given set of EOS, with strange mass of 160MeV is calculated to be 1.84 solar mass. The maximum mass for the mixed hybrid star can be increased to 2.01 [57] solar mass with s-quark mass of 300MeV and varying bag pressure of 150 MeV. Therefore the mass limit set by the observation of pulsar PRS J1614-2230 can be maintained by the mixed hybrid star having density dependent bag constant. But for this particular choice, the mixed phase region is very small. It should be mentioned here that this mass limit is only for this set of nuclear and quark matter EOSs. Using very stiff EOS sets (hadronic NL3 and quark quark NJL model) the maximum mass limit for the mixed hybrid star can be raised much higher as pointed by Lenzi & Lugones [58].

The main aim of this paper was to show the effect of magnetic field on the mixed phase EOS and its effect on the maximum mass of a star. We were also interested in showing whether simple EOS (hyperonic nuclear and MIT bag quark) can reach the limit set by PSR J1614-2230. The other most interesting fact of this calculation is that the mixed hybrid star

has radius corresponding to the maximum mass, quite different from the nuclear and strange star. They are not as compact as strange stars and their radius lies between the nuclear and strange star. It is also clear from our calculation that, if the magnetic field influence the EOS only through the Landau quantization, it has a negative effect on the matter pressure thereby making the EOS softer, and the star becomes less massive.

SUMMARY AND DISCUSSION

To summarize, we have studied the effect of magnetic field on the nuclear and quark matter EOS. We have taken into account Landau quantization effect on the charged particles of both the EOS. We have considered relativistic mean field EOS model for the nuclear matter EOS. For the quark matter EOS, we have considered simple MIT bag model with density dependent bag constant. The nuclear matter EOS is much stiffer than the quark matter EOS, and so the effect of magnetic field is much more pronounced in the quark matter. The magnetic field due to Landau quantization softens the EOS for both the matter phases since the magnetic pressure contributes negatively to the matter pressure. Here we should mention that the effect of magnetization of matter is important for strong magnetic fields, however it is believed that in NS such magnetization is small [29]. Therefore in our calculation we have neglected such effect.

Glendenning construction [47], determines the range of baryon density where both phases coexist. At densities below the mixed phase, the system is in the charge neutral hadronic phase, and for densities above the mixed phase the system is in charge neutral quark phase. We have considered density dependent bag pressure, which has been parametrized according to the Gaussian form. We have fixed the lowest value of the bag pressure to be 130MeV, known from the experiments [50]. Accordingly, we have also considered varying magnetic field. Observationally, the inferred surface magnetic field of a NS may be as high as 10^{15} G and is believed to increase at the center. As the density decreases with increasing radial distance, we have taken the parametrization of the magnetic field as a function of density, having maximum field strength at the core. Considering density dependent bag pressure and magnetic field, we construct mixed phase EOS following Glendenning construction.

We find that the effect of magnetic field is insignificant unless the surface field is of the order of 10^{14} G. Such constant magnetic field value has no effect on the nuclear matter EOS

and has very little effect on the mixed and quark matter EOS. For a varying magnetic field whose surface value is 10^{14}G but whose central value is of the order of 10^{17}G , we find significant effect on the stiffness of the EOS and also on the extend of the mixed phase region in the EOS. As the bag pressure increases the EOS for the quark phase becomes soft, and hence more the effect of magnetic field. At the central region, the bag pressure decreases but the magnetic field increases, and so their respective effect on the EOS act in the opposite direction.

The magnetic field increases as we go to much higher densities, and so the boundary between the mixed phase and the quark phase changes with increasing field strength. As the magnetic field increases, the EOS becomes less stiffer and the phase boundary between the mixed and quark phase shifts upwards to the higher density value. Towards the low density regime of the curve the effect of magnetic field is less pronounced, as the magnetic field strength is less and also the nuclear matter EOS is much stiffer. Therefore the phase boundary between the nuclear and mixed phase is less affected.

The maximum mass limit of mixed phase EOS star is also shown in this paper. We obtain a significant mixed phase region with central bag constant of 160MeV having s-quark mass of 150MeV . For higher s-quark mass (300MeV) we get a small mixed phase region with bag pressure 150MeV . For such a case we find the maximum mass for a mixed hybrid star with the given set of EOS is $2.01M_{\odot}$. The maximum mass is obtained without magnetic field effect and the introduction of the magnetic field reduces the maximum mass. Therefore the mass limit set by the observation of pulsar PRS J1614-2230 is maintained by the mixed star with varying bag constant. Our calculation also shows that the mixed hybrid star has radius (for the maximum mass) quite different from the neutron or strange star, their radius lying between the neutron and strange star.

Observationally, the surface magnetic field of most of the pulsars are in the ranges of 10^8 to 10^{12}G . Such fields have almost no effect in the EOS of matter in those stars. However, for magnetars the magnetic fields are very high ($\sim 10^{17} - 10^{18}\text{G}$). Flux conservation from progenitor stars can give rise to magnetic field of field strength 2 – 3 orders higher. The mass-radius relationship for a mixed hybrid star is quite different from the pure neutron or strange star, and so it is likely to have different observational characteristics. It is also clear that magnetars are different from normal pulsars, as they have lesser mass due to flatter EOS. It is to be mentioned here that we have only considered effect from Landau

quantization and found that they have significant effect on the mixed phase region once it is greater than 10^{14}G . Here we have not considered the effect from anomalous magnetic moment. Anomalous magnetic moment stiffens the EOS, but their effect is significant if the magnetic field strength is of the order of 10^{19}G . For such high magnetic fields the NS becomes unstable. Therefore our consideration of only the effect from Landau quantization seems alright. As the interiors of the compact stars are hidden from direct observation, we have to rely only on the observations coming from their surface. Recent developments has been made on measuring accurately the mass of compact stars but a exact measurement of their radius is still not possible [1]. The knowledge of the radius of a compact stars can really give us the hint of the matter components at the star interiors, as we have seen here that different EOS provide different mass-radius relationship.

-
- [1] Demorest, P., Pennucci, T., Ransom, S., Roberts, M., & Hessels, J. 2010, *Nature* **467**, 1081
 - [2] Freire P. C. C., Bassa C., Wex N., et al. 2010, *MNRAS*, **412**, 2763
 - [3] Glendenning N. K. *Compact Stars: Nuclear Physics, Particle Physics, and General Relativity*, (Springer-Verlag, New York, 2000)
 - [4] Weber F. *Pulsars as Astrophysical Laboratories for Nuclear and Particle Physics*, (IOP Publishing, Bristol, 1999)
 - [5] Hewish A., Bell S. J., Pilkington J. D. H., Scott P. F. and Collins R. A. 1968, *Nature* **217**, 709
 - [6] Gold T. 1968, *Nature* **218**, 731
 - [7] Akmal A., Pandharipande V. R. and Ravenhall D. G. 1998, *Phys. Rev. C* **58**, 1804
 - [8] Baldo L., Bombaci I. and Burgio G. F. 1997, *Astron. & Astrophys.* **328**, 274
 - [9] Bethe H. A. and Johnson M. B. 1974, *Nucl. Phys. A* **230**, 1
 - [10] Walecka J. D. 1974, *AstroPhys. J* **83**, 491
 - [11] Itoh, N. 1970, *Prog. Theor. Phys.* **44**, 291
 - [12] Witten E. 1984, *Phys. Rev. D* **30**, 272
 - [13] Alcock C., Farhi E. and Olinto A. 1986, *AstroPhys. J* **310**, 261
 - [14] Chodos A., Jaffe R. L., Johnson K., Thorn C. B. and Weisskopf V. F. 1974, *Phys. Rev. D* **9**, 3471

- [15] Dey M., Bombaci I., Dey J., Ray S. and Samanta B. C. 1998, Phys. Lett. B **438**, 123
- [16] Fowler G. N., Raha S and Weiner R. M. 1981, Z. Phys. C **9**, 271
- [17] Zhang Y. and Su R. K. 2003, Phys. Rev. C **67**, 015202
- [18] Alford, M., Blaschke, D., Drago, A., et al. 2007, Nature, **445**, 7
- [19] Fischer, T., Sagert, I., Pagliara, G., et al. 2010, AstroPhys. J Supp. **194**, 39
- [20] Horvath, J. E. & Lugones, G. 2004, Astron. & Astrophys. **442**, L1
- [21] Kurkela, A., Romatschke, P., & Vuorinen, A. 2010, Phys. Rev. D **81**, 105021
- [22] Kurkela, A., Romatschke, P., Vuorinen, A., & Wu, B. 2010, arXiv:1006.4062
- [23] Rüster, S. B. & Rischke, D. H. 2004, Phys. Rev. D **69**, 045011
- [24] Özel, F., Psaltis, D., Ransom, S., Demorest, P., & Alford, M. 2010, AstroPhys. J Lett. **724**, L199
- [25] Lattimer, J. M. & Prakash, M. 2010, arXiv:1012.3208
- [26] Palmer D. M., Barthelmy S., Gehrels N. et al. 2005, Nature **434**, 1107
- [27] Bocquet M., Bonazzola S., Gourgoulhon E., Novak J. 1995, Astron. & Astrophys. **301**, 757
- [28] Cardall C. Y., Prakash M. & Lattimer J. L. 2001, AstroPhys. J **554**, 322
- [29] Broderick A., Prakash M. & Lattimer J. M. 2000, AstroPhys. J **537**, 351
- [30] Chakrabarty S., Bandyopadhyay D. & Pal S. 1997, Phys. Rev. Lett. **78**, 2898
- [31] Sinha. M & Mukhopadhyay B. 2010, arXiv:1005.4995
- [32] Chen W., Zhang P. Q. & Liu L. G. 2005, Mod. Phys. Lett. A **22**, 623
- [33] Wei F. X., Mao G. J., Ko C. M., Kissinger L. S., Stoecker H. & Greiner W. 2006, Jour. Phys. G **32**, 47
- [34] Yuan Y. F. & Zhang J. L. 1999, AstroPhys. J **25**, 950
- [35] Chakrabarty S. 1996, Phys. Rev. D **54**, 1306
- [36] Felipe R. G., Martinez A. P., Rojas H. P. & Orsaria M. 2008, Phys. Rev. C **77**, 015807
- [37] Ghosh T. & Chakrabarty S. 2001, Int. Jour. Mod. Phys. D **10**, 89; 2001 Phys. Rev. D **63**, 043006
- [38] Boguta J. & Bodmer R. A. 1977, Nucl. Phys. A **292**, 413
- [39] Glendenning N. K. & Moszkowski S. A. 1991, Phys. Rev. Lett. **67**, 2414
- [40] Sugahara Y. & Toki H. 1994, Nucl. Phys. A **579**, 557
- [41] Ghosh S. K., Phatak S. C. & Sahu P. K. 1995, Z. Phys. A **352**, 457
- [42] Schaffner J. & Mishustin I. N. 1996, Phys. Rev. C **53**, 1416

- [43] Schertler K., Greiner C., Sahu P. K. & Thoma M. H. 1998, Nucl. Phys. A **637**, 451
- [44] Landau L. D. & Lifshitz E. M. *Quantum Mechanics*, (Pergamon Press, Oxford, 1965)
- [45] Chakrabarty S. & Sahu P. K. 1996, Phys. Rev. D **53**, 8
- [46] Chakrabarty S. 1995, Phys. Rev. D **51**, 4591
- [47] Glendenning N. K. 1992, Phys. Rev. D **46**, 1274
- [48] Adami C. & Brown G. E. 1993, Phys. Rep. **234**, 1 (1993); Xue-min Jin & Jennings B. K. 1997, Phys. Rev. C **55**, 1567
- [49] Blaschke D., Grigorian H., Poghosyan G., Roberts C. D. & Schmidt S. 1999, Phys. Lett. B **450**, 207
- [50] Burgio G. F., Baldo M., Sahu P. K. & Schulze H. J. 2002, Phys. Rev. C **66**, 025802
- [51] Burgio G. F., Baldo M., Sahu P. K., Santra A. B. & Schulze H. J. 2002, Phys. Lett. B **526**, 19
- [52] Shapiro S. L. & Teukolsky S. A. *Black Holes, White Dwarfs, and Neutron Stars*, (John Wiley & Sons, New York, 1983)
- [53] Negele J. W. & Vautherin D 1973, Nucl. Phys. A **207**, 298
- [54] Feynman R., Metropolis F. & Teller E. 1949, Phys. Rev. **75**, 1561
- [55] Baym G., Pethick C. & Sutherland D. 1971, AstroPhys. J **170**, 299
- [56] Lattimer J. M. & Prakash M. 2005, Phys. Rev. Lett. **94**, 111101
- [57] Mallick R. 2012, arXiv:1207:4872
- [58] Lenzi C. H. & Lugones G. 2012, arXiv:1206.4180